Earth and Planetary Science Letters 300 (2010) 33–43

Contents lists available at ScienceDirect

Earth and Planetary Science Letters

journal homepage: www.elsevier.com/locate/epsl

# Atmospheric nitrous oxide during the last 140,000 years

Adrian Schilt [a,b,*], Matthias Baumgartner [a,b], Jakob Schwander [a,b], Daphné Buiron [c], Emilie Capron [d], Jérôme Chappellaz [c], Laetitia Loulergue [c], Simon Schüpbach [a,b], Renato Spahni [a,b], Hubertus Fischer [a,b], Thomas F. Stocker [a,b]

[a] Climate and Environmental Physics, Physics Institute, University of Bern, Sidlerstrasse 5, CH-3012 Bern, Switzerland
[b] Oeschger Centre for Climate Change Research, University of Bern, CH-3012 Bern, Switzerland
[c] Laboratoire de Glaciologie et Géophysique de l'Environnement, CNRS-UJF, 38400 St Martin d'Hères, France
[d] Laboratoire des Sciences du Climat et de l'Environnement, CEA-CNRS-UVSQ, 91191 Gif-sur-Yvette, France

ARTICLE INFO

*Article history:*
Received 7 May 2010
Received in revised form 10 September 2010
Accepted 21 September 2010
Available online 20 October 2010

Editor: P. DeMenocal

*Keywords:*
greenhouse gas
radiative forcing
carbon dioxide
methane
nitrous oxide
paleo

ABSTRACT

Reconstructions of past atmospheric concentrations of greenhouse gases provide unique insight into the biogeochemical cycles and the past radiative forcing in the Earth's climate system. We present new measurements of atmospheric nitrous oxide along the ice cores of the North Greenland Ice Core Project and Talos Dome sites. Using records of several other ice cores, we are now able to establish the first complete composite nitrous oxide record reaching back to the beginning of the previous interglacial about 140,000 yr ago. On the basis of such composite ice core records, we further calculate the radiative forcing of the three most important greenhouse gases carbon dioxide, methane and nitrous oxide during more than a full glacial–interglacial cycle. Nitrous oxide varies in line with climate, reaching very low concentrations of about 200 parts per billion by volume during Marine Isotope Stages 4 and 2, and showing substantial responses to millennial time scale climate variations during the last glacial. A large part of these millennial time scale variations can be explained by parallel changes in the sources of methane and nitrous oxide. However, as revealed by high-resolution measurements covering the Dansgaard/Oeschger events 17 to 15, the evolution of these two greenhouse gases may be decoupled on the centennial time scale. Carbon dioxide and methane concentrations do not reach interglacial levels in the course of millennial time scale climate variations during the last glacial. In contrast, nitrous oxide often reaches interglacial concentrations in response to both, glacial terminations and Dansgaard/Oeschger events. This indicates, from a biogeochemical point of view, similar drivers in both temporal cases. While carbon dioxide and methane concentrations are more strongly controlled by climate changes in high latitudes, nitrous oxide emissions changes may mainly stem from the ocean and/or from soils located at low latitudes. Accordingly, we speculate that high latitudes could play the leading role to trigger glacial terminations.



## 1. Introduction

Anthropogenic emissions of nitrous oxide ($N_2O$) led to an ongoing increase of this important greenhouse gas from a preindustrial value of about 270 parts per billion by volume (ppbv) to a present-day (2008) concentration of 322 ppbv (Flückiger et al., 1999; Machida et al., 1995; WMO, 2009). $N_2O$ is naturally produced by nitrification and denitrification in terrestrial soils (about two thirds of total $N_2O$ emissions) and in the ocean (about one third of total $N_2O$ emissions) (Bouwman et al., 1993; Kroeze et al., 1999; Nevison et al., 1995). The main sink of $N_2O$ is photodissociation in the stratosphere, followed by chemical reactions with excited oxygen (Minschwaner et al., 1998). Compared to the mixing time of the atmosphere, $N_2O$ has a relatively long atmospheric lifetime of about 120 yr (Minschwaner et al., 1998; Volk et al., 1997), and accordingly shows no significant interhemispheric concentration gradient.

Thanks to the analysis of air enclosed in ice cores from polar ice sheets, paleo-atmospheric concentration records of the greenhouse gases carbon dioxide ($CO_2$) and methane ($CH_4$) are available for the entire last 800,000 yr (800 kyr) (Loulergue et al., 2008 and references therein; Lüthi et al., 2008 and references therein). For this time interval, past natural variations of $N_2O$ have been reconstructed for all interglacials and parts of glacials (Flückiger et al., 2002; Schilt et al., 2010; Sowers et al., 2003; Spahni et al., 2005). In addition, there exist $N_2O$ records covering selected Dansgaard/Oeschger (DO) events (Flückiger et al., 1999, 2004). DO events are millennial time scale climate variations during the last glacial as recorded in Greenland ice cores (e.g. Dansgaard et al., 1984; NGRIP Members, 2004) with counterparts visible over a wide spread of latitudes (e.g. Bond et al.,

* Corresponding author. Climate and Environmental Physics, Physics Institute, University of Bern, Sidlerstrasse 5, CH-3012 Bern, Switzerland. Tel.: +41 31 631 44 76; fax: +41 31 631 87 42.
*E-mail address:* schilt@climate.unibe.ch (A. Schilt).

0012-821X/$ – see front matter © 2010 Elsevier B.V. All rights reserved.
doi:10.1016/j.epsl.2010.09.027

1993; Voelker, 2002). However, $N_2O$ records have remained fragmentary due to the occurrence of in situ artefacts (Section 3), which has so far precluded to reconstruct the evolution of the $N_2O$ concentration in the course of a full glacial–interglacial cycle. New measurements along the ice cores of the Talos Dome (TD, Antarctica, 72°47′ S, 159°04′ E) and North Greenland Ice Core Project (NGRIP, Greenland, 75°06′ N, 42°20′ W) sites now fill existing gaps in the $N_2O$ records of the last 140 kyr.

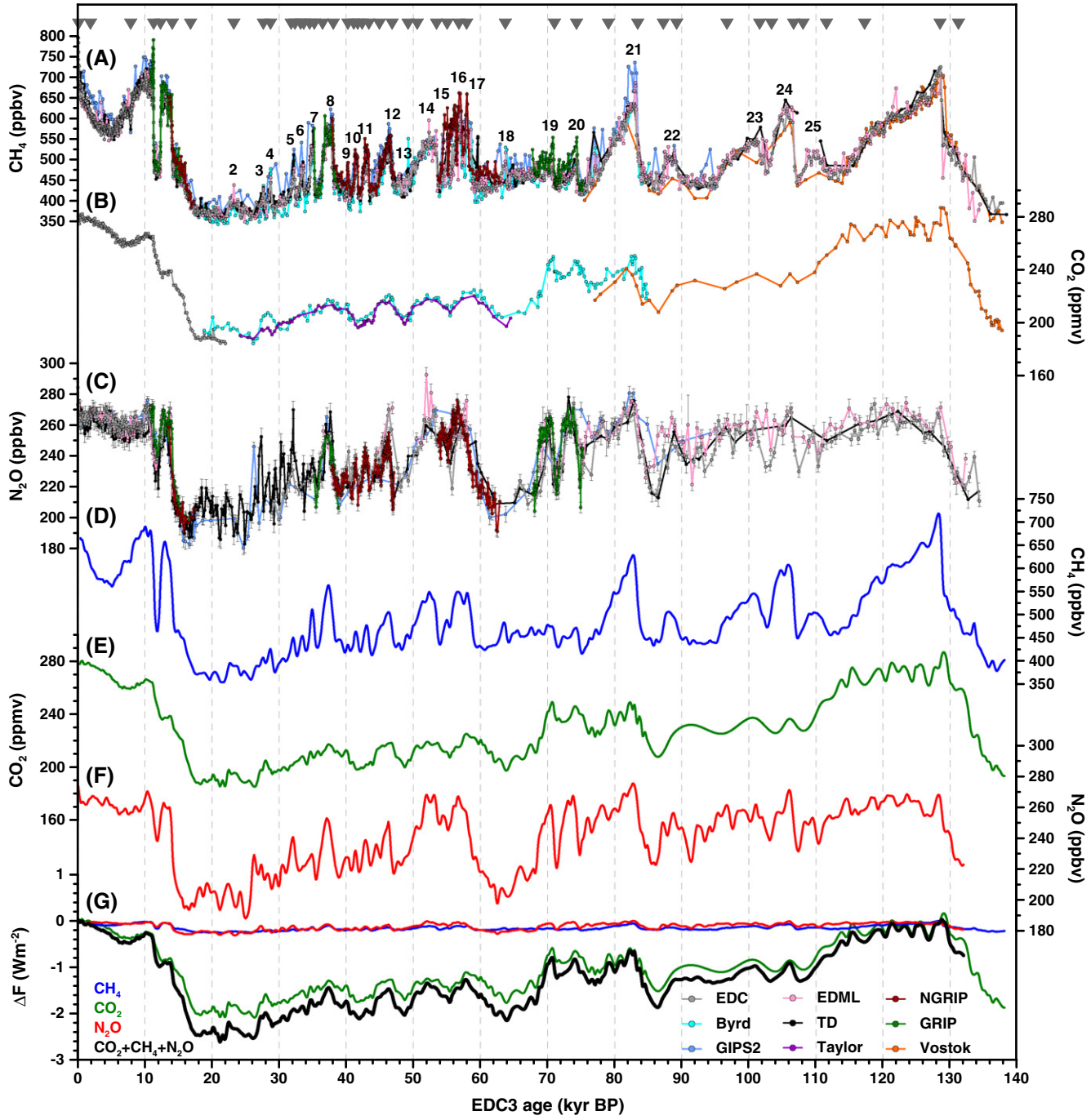


**Fig. 1.** Greenhouse gas records covering the last 140 kyr on the EDC3 time scale (Loulergue et al., 2007). (A) Synchronised $CH_4$ records of EDC (Flückiger et al., 2002; Monnin et al., 2001; Spahni et al., 2005), EDML (Capron et al., 2010; EPICA Community Members, 2006; and new data), NGRIP (Flückiger et al., 2004; Huber et al., 2006; and new data), Byrd (Blunier et al., 1998), TD (Buiron et al., 2010; Stenni et al., submitted for publication), GRIP (Blunier et al., 1998; Chappellaz et al., 1993, 1997; Dällenbach et al., 2000; Flückiger et al., 2004), GISP2 (Brook et al., 1996, 2000) and Vostok (Petit et al., 1999). The grey triangles on top of the $CH_4$ records indicate the locations of the tie points used for the $CH_4$ synchronisation (see Appendix A.4). Numbers denote DO events. (B) $CO_2$ records from EDC (Monnin et al., 2001, 2004), Byrd (Ahn and Brook, 2007, 2008), Taylor Dome (Indermühle et al., 2000) and Vostok (Pepin et al., 2001; Petit et al., 1999). (C) $N_2O$ records from EDC (Flückiger et al., 2002; Spahni et al., 2005; Stauffer et al., 2002), EDML (Schilt et al., 2010), NGRIP (Flückiger et al., 2004; and new data), TD (new data), GRIP (Flückiger et al., 1999) and GISP2 (Sowers et al., 2003). (D) $CH_4$ smoothing spline, cutoff period of 1000 yr (Enting, 1987), only EDC $CH_4$ data used. (E) $CO_2$ smoothing spline, cutoff period of 1000 yr (Enting, 1987), all data used. (F) $N_2O$ smoothing spline, cutoff period of 1000 yr (Enting, 1987), all data used. (G) Radiative forcing (relative to the year 1750) of $CH_4$ (blue), $CO_2$ (green), $N_2O$ (red) and all three greenhouse gases together (black) calculated according to Ramaswamy et al. (2001). The legend at the lower right corner indicates the colour code for the ice core measurements.

## 2. Data records

We present 287 $N_2O$ measurements performed along the TD ice core reaching back to about 140 kyr before present (140 kyr BP) covering Termination 2, Marine Isotope Stage (MIS) 5.5, the last glacial, Termination 1 and the Holocene (Fig. 1). On the TALDICE1 time scale (Buiron et al., 2010), the mean time resolution is about 1150 yr between 140 and 40 kyr BP, and better than 200 yr for the last 40 kyr. In addition, we present 164 $N_2O$ measurements performed along the NGRIP ice core covering the DO events 17 to 15 from 63 to 55 kyr BP and parts of Termination 1 (Figs. 1 and 2). These new NGRIP measurements provide a mean time resolution of 72 yr on the GRIP2001/SS09sea age scale (Huber et al., 2006; Johnsen et al., 2001; NGRIP Members, 2004).

For synchronisation purposes we also use new $CH_4$ data (Fig. 1). First, 31 new $CH_4$ measurements cover for the first time parts of Termination 1 along the NGRIP ice core (same samples as for $N_2O$ measurements). Second, we use 197 new $CH_4$ measurements performed along the ice core of the European Project for Ice Coring in Antarctica (EPICA) Dronning Maud Land (EDML, Antarctica, 75°00′ S, 00°04′ E) site. These measurements complete the EDML $CH_4$ record (Capron et al., 2010; EPICA Community Members, 2006) back to 140 kyr BP with a mean time resolution of better than 200 yr on the EDML1 time scale (Loulergue et al., 2007; Ruth et al., 2007).

We further use a new TD dust record reaching back to 140 kyr BP, with some gaps during the Holocene and the last glacial (Figs. 3 and 4).

For the TD $N_2O$ measurements the standard deviation ($1\sigma$) is 5.6 ppbv as discussed in Appendix A.1. The standard deviation of our $CH_4$ measurements is 10 ppbv (Chappellaz et al., 1997). See Appendices A.1 and A.3 for details about the measurement techniques for $N_2O$, $CH_4$ and dust. Appendix A.2 describes the offset corrections applied to parts of the $N_2O$ and $CH_4$ measurements.

## 3. $N_2O$ artefacts

$N_2O$ records reconstructed from polar ice cores occasionally show elevated values exceeding atmospheric concentrations (e.g. Flückiger et al., 2004; Schilt et al., 2010; Sowers, 2001; Spahni et al., 2005). These $N_2O$ artefacts originate from in situ production of $N_2O$ in the ice, likely due to microbial activity (Miteva et al., 2007; Rohde et al., 2008).

In order to detect measurements affected by artefacts in the NGRIP $N_2O$ record we use the artefact detection algorithm already applied to earlier NGRIP $N_2O$ records (Flückiger et al., 2004). This algorithm is only suitable for high-resolution records, and it iteratively excludes values which deviate more than 8 ppbv from a smoothing spline with a cutoff period of 600 yr (Enting, 1987) calculated through the data. This algorithm is designed to empirically identify values outside the analytical precision that cannot be explained by atmospheric $N_2O$ variability taking into account the long lifetime of $N_2O$.

Along the EDML and EPICA Dome C (EDC, Antarctica, 75°06′ S, 123°21′ E) ice cores, $N_2O$ measurements performed on ice samples with dust concentrations above an empirical threshold of 300 parts per billion by weight (ppbw) have been defined as affected by artefacts, because nearby measurements on such samples showed unusually high $N_2O$ concentrations and large scatter (Schilt et al., 2010; Spahni et al., 2005). Note that this does not imply that in situ production of $N_2O$ in the ice is directly related to the dust concentration itself. Rather, the responsible impurities and/or bacterial cells may reach the EDML and EDC sites by the same pathway as the dust particles.

Along the TD ice core, dust concentrations are almost always below this empirical threshold as applied to the EDML and EDC ice cores. The only exception to that are short intervals found in ice of MIS 2, where dust concentrations are above 300 ppbw (Fig. 3). Nevertheless, during these intervals, the TD $N_2O$ record generally shows substantially lower values and lower scatter than the EDML and EDC $N_2O$ records corresponding to the same age (Fig. 4). Looking at ice cores from Greenland, artefacts do not show a correlation with impurities such as e.g. dust and calcium. Instead, they preferentially occur in depth intervals with fast changing concentrations of impurities mainly located at the boundaries of DO events (Flückiger et al., 2004). Given the fact that concentrations of impurities along the TD ice core are

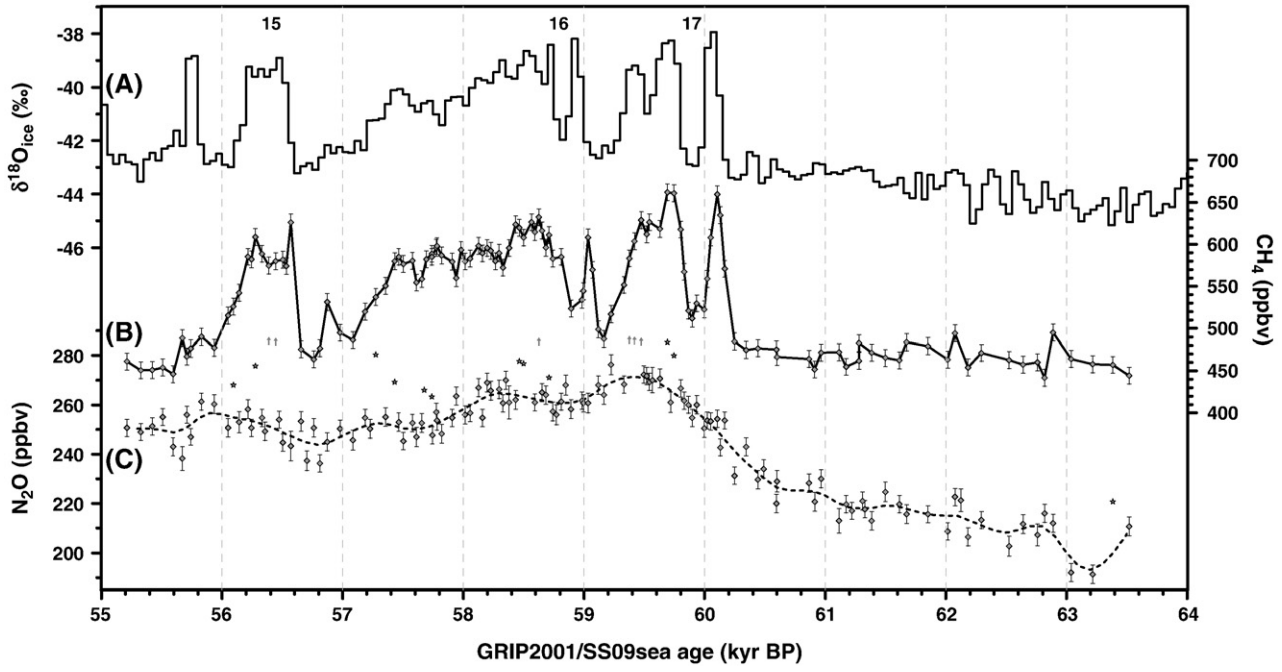


**Fig. 2.** $\delta^{18}O_{ice}$, $CH_4$ and $N_2O$ during the DO events 17 to 15. (A) NGRIP $\delta^{18}O_{ice}$, a qualitative proxy for Greenland temperature variations (NGRIP Members, 2004). As investigated on the basis of $\delta^{15}N$ measurements on atmospheric nitrogen, Greenland temperature shows very fast increases of 12, 9 and 10 °C at the beginning of the DO events 17, 16 and 15, respectively (Huber et al., 2006). (B) NGRIP $CH_4$ characterized by nearly in phase increases with $\delta^{18}O_{ice}$ (Huber et al., 2006). (C) NGRIP $N_2O$ (new data). Measurements affected by artefacts (stars, values exceeding the y-axis are indicated by arrows) are excluded by the use of the artefact detection algorithm described in Flückiger et al. (2004). The dashed line shows a smoothing spline with a cutoff period of 600 yr (Enting, 1987). All data are plotted on the GRIP2001/SS09sea time scale (Huber et al., 2006; Johnsen et al., 2001; NGRIP Members, 2004).

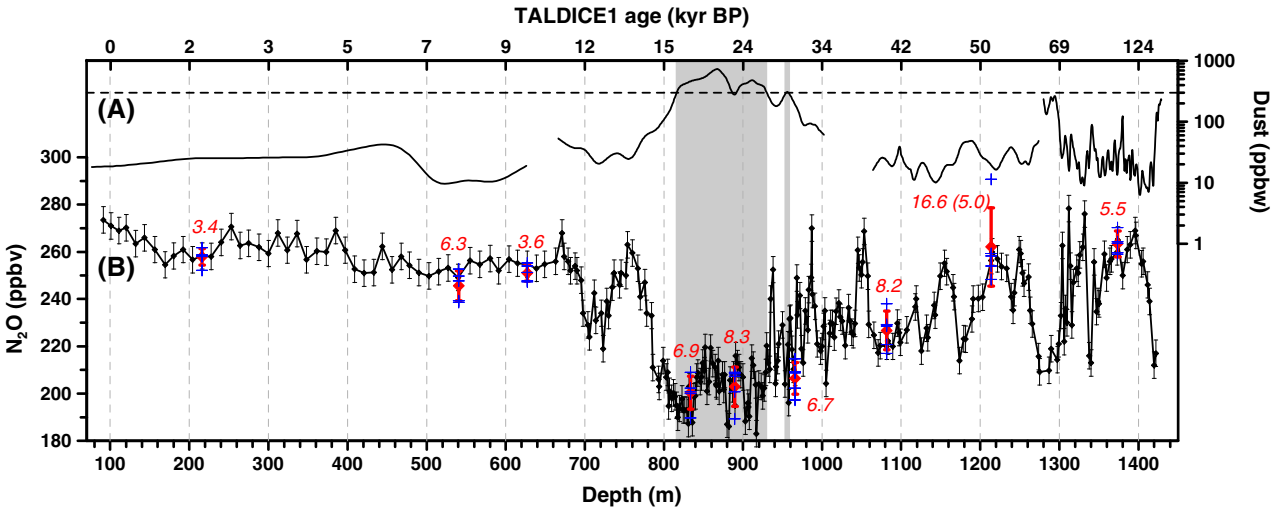


**Fig. 3.** TD dust and $N_2O$ on their respective depth scale. (A) Solid line: TD dust concentration (smoothing spline with cutoff period of 2000 yr according to Enting (1987), new data). Dashed line: concentration threshold of 300 ppbw as applied to the EDML and EDC ice cores. Grey shaded areas: depth intervals with a dust concentration exceeding the threshold of 300 ppbw. (B) Black: TD $N_2O$ (new data). Red: mean and standard deviation of five adjacent samples for each depth level (see Appendix A.1). Blue crosses show the single measurements and red italic numbers indicate the standard deviations in ppbv. The number in brackets is the standard deviation calculated without taking into account the highest measurement out of the five adjacent samples for this depth. The top x-axis indicates the TALDICE1 gas age (Buiron et al., 2010).

orders of magnitude lower and do not show large and rapid changes at the boundaries of DO events, it appears to be rather unlikely that a similar relationship between impurities and $N_2O$ artefacts as observed along ice cores from Greenland holds also true for this Antarctic ice core. In view of these results, we suggest that the TD ice core reveals a $N_2O$ record of atmospheric origin over its full length (including the late last glacial), regardless of the fact that dust concentrations sometimes exceed the empirical threshold of 300 ppbw as applied to the EDML and EDC ice cores. However, we cannot strictly exclude a partial contamination of the TD $N_2O$ record during any time interval. In particular, the TD $N_2O$ record during MIS 2 may serve only as an upper concentration limit until verified by $N_2O$ records from other ice cores (note that no indications exist for artefacts leading to values below the atmospheric concentration). Further, the TD $N_2O$ record may be

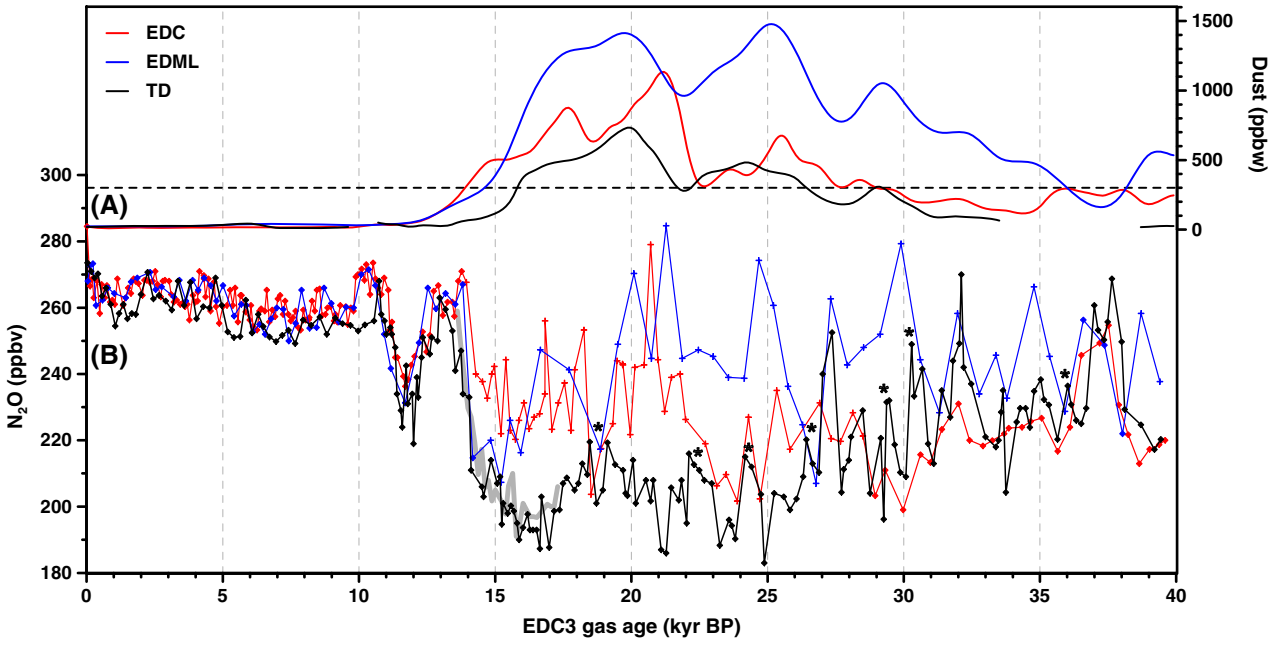


**Fig. 4.** Comparison of dust and $N_2O$ from the EDC, EDML and TD ice cores. (A) Dust records of EDC (Lambert et al., 2008), EDML (EPICA Community Members, 2006) and TD (new data). Shown are smoothing splines with a cutoff period of 2000 yr (Enting, 1987). The dashed line shows the concentration threshold of 300 ppbw as applied to the EDML and EDC ice cores. (B) $N_2O$ records of EDML (Schilt et al., 2010), EDC (Flückiger et al., 2002; Spahni et al., 2005; Stauffer et al., 2002) and TD (new data). Crosses mark EDC and EDML measurements defined as affected by artefacts, measurements marked with diamonds are thought to represent atmospheric concentrations. Asterisks mark events in the TD $N_2O$ record which do not have a counterpart in $CH_4$. Note that between 26 and 16 kyr BP, $CH_4$ only shows very small variations in response to DO event 2 (Fig. 1). Dust and $N_2O$ records are shown on the ($CH_4$ synchronised) EDC3 gas age scale (Loulergue et al., 2007), wherefore dust and gas measurements from each ice core plotted at the same age stem from the same depth. During time intervals with TD dust concentrations above the threshold of 300 ppbw, the mean $N_2O$ concentrations of EDC, EDML and TD are 229.1, 246.3 and 203.3 ppbv, respectively. The standard deviations during these time intervals are 16.5, 18.0 and 10.0 ppbv, respectively. Note that the TD $N_2O$ measurements at the end of MIS 2 and during Termination 1 are in good agreement with the measurements performed along the NGRIP ice core (grey line in the background).

questionable for some of the fast variations found during MIS 3 and 2, since some of these variations do not have a counterpart in $CH_4$ and, thus, do not correspond to a DO event (see asterisks in Fig. 4). Higher time resolution and verification with $N_2O$ records from other ice cores will help to draw final conclusions regarding these fast $N_2O$ variations during MIS 3 and 2.

Overall, we observe a satisfactory agreement between TD and other atmospheric $N_2O$ records during overlapping time intervals during the last 140 kyr (Figs. 1, 4, and 7 and Appendix A.2), increasing our confidence in the atmospheric origin of the TD $N_2O$ record.

## 4. Results

### 4.1. Glacial $N_2O$ variations

The new NGRIP and TD measurements reproduce the evolution of atmospheric $N_2O$ during Termination 1 and the Holocene as revealed by earlier studies (Flückiger et al., 1999, 2002; Schilt et al., 2010; Sowers et al., 2003), and fill gaps in the existing $N_2O$ records of the last glacial (Fig. 1). In particular, the TD measurements allow for a reconstruction of the atmospheric $N_2O$ concentration during MIS 2 including the Last Glacial Maximum (LGM), where we observe a concentration of $202 \pm 8$ ppbv (mean and standard deviation from 25 to 15 kyr BP). The records confirm the glacial–interglacial concentration increase from about 200 ppbv during the LGM to about 270 ppbv during the early Holocene (Flückiger et al., 1999). Further, the TD $N_2O$ record reveals large variations in response to the DO events of the last glacial. The amplitudes of $CH_4$ variations decrease approximately linearly from the DO events 8 to 2. This trend is probably caused by (i) reduced summer insolation in the tropical and mid-northern latitudes (Brook et al., 1996; Flückiger et al., 2004), (ii) spreading ice sheets increasingly covering boreal source regions, and (iii) decreasing temperature amplitudes in the high northern latitudes for the DO events 8 to 2. The last hypothesis is not supported by measurements of the oxygen isotopic composition of precipitation ($\delta^{18}O_{ice}$, a qualitative proxy for temperature variations) along Greenland ice cores, since such measurements do not show decreasing amplitudes for the DO events 8 to 2 (NGRIP Members, 2004). However, the real temperature changes could differ from the $\delta^{18}O_{ice}$ temperature proxy, e.g. due to changing origin or seasonality of precipitation (Masson-Delmotte et al., 2005). Further, the temperature changes over Greenland may not completely be representative for the temperature changes in most of the northern hemisphere, and Greenland ice cores may primarily record wintertime temperature changes (Denton et al., 2005), which are less important for the emissions of greenhouse gases. All three hypothesis suppose that $CH_4$ emissions (from wetlands) located at high northern latitudes are of primary importance for $CH_4$ variations in response to DO events, which is supported by studies of the interpolar gradient and hydrogen isotopic composition of $CH_4$ (Bock et al., 2010; Dällenbach et al., 2000). Since the $N_2O$ response to the DO events 8 to 2 does not show a decrease in amplitudes like $CH_4$, we suggest that the observed $N_2O$ variations are driven by marine and/or terrestrial emissions from low latitudes (Schilt et al., 2010; Schmittner and Galbraith, 2008). Indeed, reconstructions of the isotopic composition of atmospheric oxygen point to large changes in the hydrological cycle and, thus, in the photosynthetic capacity of the terrestrial surface in concert with the DO events during the last glacial (Landais et al., 2007; Severinghaus et al., 2009). These changes are mainly located at low latitudes and they may affect the $N_2O$ emissions from soils. On the other hand, reconstructions of denitrification rates in the Arabian Sea and in the Eastern Tropical North Pacific also show strong reactions to DO events (Emmer and Thunell, 2000; Suthhof et al., 2001). These two important lower latitude regions for marine $N_2O$ emissions alone could be responsible for substantial changes in the atmospheric $N_2O$ concentration.

### 4.2. $N_2O$ during the DO events 17 to 15

Figure 2 presents the high-resolution NGRIP $N_2O$ record covering the DO events 17 to 15, along with the NGRIP $CH_4$ record (Huber et al., 2006) and the NGRIP $\delta^{18}O_{ice}$ record (NGRIP Members, 2004). As noted for other DO events (Flückiger et al., 2004), the new NGRIP $N_2O$ record generally follows Greenland temperature and $CH_4$, reaching concentrations of about 260 to 275 ppbv during interstadials. However, $N_2O$ differs from Greenland temperature and $CH_4$ in its temporal evolution. In the long-lasting stadial preceding DO event 17, the slow $N_2O$ increase (which occurs in concert with increasing $\delta^{18}O_{ice}$ but constant $CH_4$) starts from around 200 ppbv. In the course of the last glacial–interglacial cycle, such low $N_2O$ concentrations have otherwise only been reconstructed for MIS 2 (Fig. 1). Several hundred years before the rapid increase of $\delta^{18}O_{ice}$ and $CH_4$ corresponding to the onset of DO event 17, the increase rate of $N_2O$ changes from ~0.8 ppbv/century to ~4.1 ppbv/century. This increase rate of ~4.1 ppbv/century is still about 10 times slower than the anthropogenic increase rate of the last 50 yr (Khalil et al., 2002). The early increase of $N_2O$ compared to $\delta^{18}O_{ice}$ and $CH_4$ points to changes in the biogeochemical cycles related to $N_2O$ occurring hundreds of years before the rapid temperature increase in Greenland. Note, however, that Bock et al. (2010) also observe a change in the hydrogen isotopic composition of $CH_4$ (without considerably affecting the $CH_4$ concentration) about 500 yr before DO event 8, pointing to changes of boreal wetlands before the rapid temperature increase in Greenland. An early increase of $N_2O$ has also been reproduced for other long-lasting DO events (e.g. 20, 19, 12 and 8), while shorter DO events (e.g. 11 and 10) show a rather synchronous increase of $CH_4$ and $N_2O$ (Flückiger et al., 2004). It has been shown that a substantial Antarctic warming precedes each DO event observed in Greenland (EPICA Community Members, 2006). However, a causal relationship between this early warming in the south and the early increase of $N_2O$ can be excluded because of the different timing (Flückiger et al., 2004). Recent model simulations of Schmittner and Galbraith (2008) rather suggest that long-term adjustment of the nitrate and oxygen content in the thermocline after the collapse of the Atlantic Meridional Overturning Circulation (AMOC) could be responsible for the early increase of $N_2O$.

The maximum $N_2O$ concentration during DO event 17 is on the order of the preindustrial Holocene value (Flückiger et al., 1999). As for other DO events, $N_2O$ reaches the maximum several hundred years later than $\delta^{18}O_{ice}$ and $CH_4$. This lag is likely caused by the relatively long lifetime of $N_2O$, and does not necessarily mean that $N_2O$ emissions continued to increase while $CH_4$ emissions already reached a stable level (Flückiger et al., 2004).

In the course of the DO events 17 and 16, the Greenland $\delta^{18}O_{ice}$ record is characterized by fast centennial time scale temperature variations between stadials and interstadials. While $CH_4$ clearly responds to every single variation in the $\delta^{18}O_{ice}$ record within a few decades (Huber et al., 2006), $N_2O$ remains on a typical interstadial level even when $\delta^{18}O_{ice}$ and $CH_4$ drop to stadial levels (Fig. 2). The question is whether the longer atmospheric lifetime of $N_2O$ compared to the atmospheric lifetime of $CH_4$ can lead to the observed differences between the two greenhouse gas records. To address this question, we calculate the $CH_4$ emissions required to explain the reconstructed $CH_4$ concentration under the assumption of a constant lifetime which is set to 10 yr (Chappellaz et al., 1997; Martinerie et al., 1995). Due to this relatively short lifetime, $CH_4$ emissions and $CH_4$ concentration change nearly in parallel. Assuming that $N_2O$ emissions are proportional to the $CH_4$ emissions, the corresponding hypothetical $N_2O$ emissions and the deduced hypothetical $N_2O$ concentration can be calculated, whereby the lifetime of $N_2O$ is set to 120 yr (Minschwaner et al., 1998; Volk et al., 1997). The hypothetical $N_2O$ concentration follows, although in a smoothed way, the rapid changes in $\delta^{18}O_{ice}$ and $CH_4$, and thus contradicts the NGRIP $N_2O$ record which does not respond to the changes in $\delta^{18}O_{ice}$ and $CH_4$ (Fig. 5). Hence, the relatively long lifetime

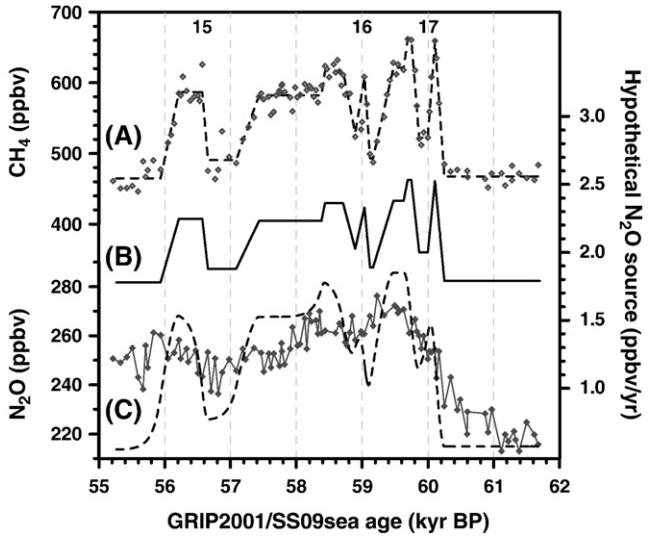


**Fig. 5.** Influence of the atmospheric lifetime on the $N_2O$ concentration during the DO events 17 to 15. (A) NGRIP $CH_4$ (diamonds, Huber et al., 2006) with approximated variations (dashed line). (B) Hypothetical $N_2O$ source calculated by scaling the $CH_4$ source (not shown, calculated from the approximated $CH_4$ variations) in such a way, that the hypothetical $N_2O$ concentration agrees with the reconstructed values in the stadial before DO event 17. (C) NGRIP $N_2O$ (diamonds, new data) with hypothetical $N_2O$ concentration (dashed line) calculated from the hypothetical $N_2O$ source. The atmospheric lifetimes of $CH_4$ and $N_2O$ are set to 10 and 120 yr, respectively, and held constant.

of $N_2O$ can only partly explain the slowly varying and high $N_2O$ concentration. The assumption of parallel variations in the emissions of $CH_4$ and $N_2O$ in response to the centennial time scale climate variations during the DO events 17 and 16 has thus to be rejected.

In the stadial between the DO events 16 and 15, $N_2O$ reaches values of about 240 ppbv. During the subsequent increase into DO event 15, $N_2O$ again does not show any direct response to the fast increase in $\delta^{18}O_{ice}$ and $CH_4$, and reaches its maximum of about 260 ppbv several hundred years later than $CH_4$ (Fig. 2).

As discussed in Section 4.1, the high northern latitudes may play an important role for $CH_4$ emissions in response to DO events. Assuming that these high northern latitude sources are also responsible for the centennial time scale $CH_4$ variations observed during the DO events 17 and 16, we suggest that terrestrial $N_2O$ emissions from these regions contribute, if at all, weakly to the observed variations in the $N_2O$ concentration. Accordingly, the insensitivity of $N_2O$ concentrations to centennial time scale temperature and $CH_4$ variations as observed along the NGRIP ice core during the DO events 17 and 16 could add weight to the hypothesis that atmospheric $N_2O$ concentrations observed in response to DO events are mainly driven by marine and/or terrestrial $N_2O$ emissions from low latitudes (Schilt et al., 2010; Schmittner and Galbraith, 2008).

## 5. Discussion

### 5.1. Radiative forcing during the last 140 kyr

Detailed knowledge of the past atmospheric greenhouse gas concentrations and thus the radiative forcing of the atmosphere is indispensable for modelling studies of the Earth's climate system. In order to provide records of the three most important greenhouse gases on a common time scale, we assemble and synchronise records of $CO_2$, $CH_4$ and $N_2O$ from numerous ice cores (including new and published data), and calculate the radiative forcing (Fig. 1).

First, we present a composite $CO_2$ record (smoothing spline with a cut off period of 1000 yr calculated according to Enting (1987)) covering the last 140 kyr and consisting of earlier published records from the EDC, Taylor Dome (Antarctica, 77°48′ S, 158°43′ E), Byrd (Antarctica, 80°01′ S, 119°31′ W) and Vostok (Antarctica, 78°28′ S, 106°50′ E) ice cores. Second, we calculate a smoothing spline with a cutoff period of 1000 yr (Enting, 1987) through the EDC $CH_4$ record. We do not use a composite record for $CH_4$ since doing so would add uncertainties rather than new information. Note that the $CH_4$ smoothing spline represents a southern hemisphere signal, while the interpolar gradient of $CH_4$ has been found to reach values of up to about 50 ppbv (Chappellaz et al., 1997; Dällenbach et al., 2000). Third, we establish a composite $N_2O$ record consisting of measurements obtained from the EDC, EDML, TD and NGRIP ice cores, as well as from the ice cores of the Greenland Ice Core Project (GRIP, Greenland, 72°34′ N, 37°38′ W) and the Greenland Ice Sheet Project 2 (GISP2, Greenland, 72°36′ N, 38°30′ W) sites. The composite $N_2O$ record (smoothing spline with a cut off period of 1000 yr calculated according to Enting (1987)) now covers the last 140 kyr without gaps, owing to the new measurements along the TD ice core. In order to put $CO_2$, $CH_4$ and $N_2O$ records from different ice cores on the EDC3 time scale (Loulergue et al., 2007), we perform a $CH_4$ synchronisation (Appendix A.4).

The records enable a comprehensive insight into the radiative forcing of $CO_2$, $CH_4$ and $N_2O$ during the last 140 kyr. The radiative forcing as shown in Figure 1 is calculated according to Ramaswamy et al. (2001) relative to the year 1750 (preindustrial forcing). As already noted in previous work (e.g. Chappellaz et al., 1990; Leuenberger and Siegenthaler, 1992), $CH_4$ and $N_2O$ contribute approximately equally to the (natural) global radiative forcing during the last 140 kyr, but their contribution is of secondary importance compared to the radiative forcing of $CO_2$ ($CH_4$ and $N_2O$ together contribute about 20% to the total change in the radiative forcing of all greenhouse gases over Termination 1). The provided smoothing splines through the $CO_2$, $CH_4$ and $N_2O$ composite records allow for an insight into long-term evolutions of the paleo-atmospheric greenhouse gas concentrations, however, there are limitations to study detailed responses on centennial to millennial time scales. For this we would rather suggest to rely on high-resolution greenhouse gas measurements from one single ice core.

### 5.2. Comparison of millennial time scale climate variations and glacial terminations

Investigation of natural mechanisms causing the Earth's climate system to shift between cooler and warmer climate states could provide crucial information to improve projections of the climate in the future. For past natural climate variations on glacial–interglacial time scales, the strong imprint of insolation, which becomes apparent when looking at frequency spectra of climate records and insolation (Hays et al., 1976), shows that external forcing plays an important role or may act as a trigger. While it is clear that external forcing can, however, not quantitatively explain the global changes in the radiative forcing necessary for glacial–interglacial transitions, the interaction of insolation with climate drivers on Earth (such as atmosphere, cryosphere, land, and ocean) leading to a sufficient internal amplification is still not completely understood. As demonstrated by the calculation of the radiative forcing (Section 5.1), $CO_2$ strongly feeds back on global climate, while $CH_4$ and $N_2O$ contribute less to the total radiative forcing of greenhouse gases on glacial–interglacial and millennial time scales. Therefore, rather than considering $CH_4$ and $N_2O$ as first-order climate drivers, we here understand their atmospheric concentrations as globally integrated indicators of changes in the biogeochemical cycles. Thereby, variations in $CH_4$ are thought to mainly indicate changes in boreal and tropical wetland emissions, and thus changes in precipitation patterns, temperature, sea level and ice sheet extent (e.g. Berrittella and van Huissteden, 2009; Brook et al., 2000; Bubier and Moore, 1994). Variations in $N_2O$ are thought to be caused by changes in

marine and/or terrestrial emissions from low latitudes (e.g. Schilt et al., 2010; Schmittner and Galbraith, 2008). While some studies suggest quite stable atmospheric sinks for $CH_4$ and $N_2O$ over time (Crutzen and Bruhl, 1993; Martinerie et al., 1995), other investigations indicate that variations in the sinks of the two greenhouse gases could still have the potential to strongly influence the atmospheric budgets (e.g. Fischer et al., 2008; Kaplan et al., 2006).

During the last glacial, records from Antarctic ice cores reveal numerous temperature variations on a millennial time scale. Such Antarctic Isotope Maxima (AIM) events (EPICA Community Members, 2006) correspond to a slow and steady warming around Antarctica followed by a similar cooling, the latter being initiated by a fast increase in the temperature recorded in Greenland ice cores, i.e. a DO event (EPICA Community Members, 2006). This interplay of southern and northern temperatures may be driven by changes in the AMOC and is known as the bipolar seesaw (Broecker, 1998; Stocker, 1998; Stocker and Johnsen, 2003). Wolff et al. (2009) have looked at a proxy for Antarctic temperature variations and have found that initial phases of AIM events and glacial terminations are indistinguishable regarding their temperature evolution. According to Wolff et al. (2009), both, AIM events and glacial terminations, are led by a warming in the southern hemisphere. In case of glacial terminations no northern control sets in, allowing southern warming (and associated atmospheric $CO_2$) to increase beyond a point of no return that pushes climate into an interglacial state. In turn, during AIM events, the AMOC strengthens which leads to a cooling in the southern hemisphere and an accompanying decline in atmospheric $CO_2$, finally resulting in a stadial climate.

Here, we look at greenhouse gas concentrations and add a biogeochemical point of view to this discussion. Comparing the greenhouse gas concentrations during the last 140 kyr as recorded in response to DO/AIM events and glacial terminations, we observe that maximum $CH_4$ and $CO_2$ concentrations during DO/AIM events never reach values as high as at the end of Termination 1 and Termination 2. (Fig. 1). In contrast, high interglacial $N_2O$ concentrations are very common also during DO events. In order to highlight one particular case of similarities in $N_2O$ responses to DO events and glacial terminations, we compare the evolution of $N_2O$ during the DO events 17 to 15 and Termination 1 (Fig. 6). The former time interval corresponds to the transition from MIS 4 to 3 (Section 4.2), and thus to one of the strongest climate changes during the last glacial not leading to an interglacial. A detailed comparison of the transition from MIS 4 to 3 and Termination 1 can also be found in Liu et al. (2010). Remarkably, the $N_2O$ records of the two selected time intervals evolve virtually identically until 3000 yr after the beginning of the $N_2O$ rise, when $N_2O$ concentrations decrease at the end of DO event 16 on the one hand or increase into the Preboreal on the other hand.

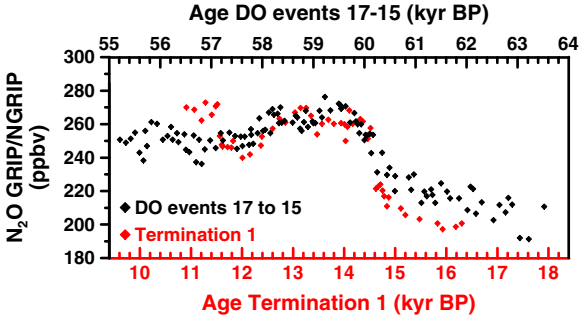


**Fig. 6.** Comparison of $N_2O$ during Termination 1 and the transition from MIS 4 to 3 corresponding to the DO events 17 to 15. Red: GRIP $N_2O$ (Flückiger et al., 1999) shown on the SS09 time scale (Dansgaard et al., 1993; Johnsen et al., 2001) with gas ages according to Schwander et al. (1997). Black: NGRIP $N_2O$ (new data) shown on the GRIP2001/SS09sea time scale (Huber et al., 2006; Johnsen et al., 2001; NGRIP Members, 2004). Both x-axes span 9 kyr.

Such similarities as for the evolution of $N_2O$ in response to the transition from MIS 4 to 3 and Termination 1 are not apparent for $CH_4$ and $CO_2$. The baseline values prior to the two transitions differ by about 50 ppbv for $CH_4$ and by about 20 ppmv for $CO_2$. Further, as for DO/AIM events in general, $CH_4$ and $CO_2$ concentrations do not reach interglacial levels during the transition from MIS 4 to 3, in contrast to $N_2O$ concentrations. From the point of view of $N_2O$ the DO events 17 to 15 could be classified as "interglacial". Our observations suggest that the mechanisms leading to DO/AIM events and glacial terminations could have the same influence on the sources (and sinks) of $N_2O$, while the responses of $CH_4$ and $CO_2$ clearly differ for the two types of transitions. Since we think that $N_2O$ is strongly influenced by the ocean and soils located at low latitudes, while $CH_4$ and $CO_2$ may also be driven by changes occurring at high latitudes of both hemispheres (in addition to important contributions from the tropics), we finally speculate that processes located at high latitudes are a determining factor on whether an ongoing transition leads to an interglacial or not.

## 6. Conclusions

New measurements along the TD ice core provide for the first time an entire atmospheric $N_2O$ record during MIS 2, including the LGM which is characterized by a mean $N_2O$ concentration of $202 \pm 8$ ppbv. The TD $N_2O$ record shows large variations in response to the DO events 8 to 2, while $CH_4$ amplitudes during these DO events decrease towards the LGM. We therefore suggest that $N_2O$ emissions are not regulated by the very same parameters responsible for the amplitude modulation of $CH_4$ changes in response to DO events. This could point to a predominance of marine and/or terrestrial $N_2O$ emissions from low latitudes (Schilt et al., 2010; Schmittner and Galbraith, 2008). In view of the large $N_2O$ variations in response to the DO events around the end of the last glacial, $N_2O$ could become a tool for synchronising ice cores during this crucial time interval where only minor changes in $CH_4$ occur. However, $N_2O$ measurements affected by artefacts could complicate the picture.

High-resolution $N_2O$ measurements along the NGRIP ice core covering the DO events 17 to 15 confirm that $N_2O$ starts to increase hundreds of years before the rapid increase in Greenland temperature and $CH_4$ at the beginning of long-lasting DO events (Flückiger et al., 2004). While a large part of the $CH_4$ and $N_2O$ responses to millennial time scale variations during the last glacial can be explained by parallel changes in the sources of the two greenhouse gases, our data show that $CH_4$ and $N_2O$ emissions evolved independently in the course of centennial time scale variations during the DO events 17 and 16.

A composite $N_2O$ record gives for the first time a complete overview of the evolution of atmospheric $N_2O$ back to the beginning of the previous interglacial. By the additional use of numerous $CH_4$ and $CO_2$ ice core records put on a common time scale, we calculate the radiative forcing of these three most important long-living greenhouse gases for the last 140 kyr. Although the provided smoothing splines do not resolve very detailed variations on centennial to millennial time scales, they may be useful for future modelling studies focussing on glacial–interglacial time scales.

The comparison of large climate transitions has revealed that Antarctic temperature evolves similarly during initial phases of DO/AIM events and glacial terminations (Wolff et al., 2009). Because we find that (during the last 140 kyr) $N_2O$ concentrations during DO events often reach levels similar to those at the end of glacial terminations, while $CH_4$ and $CO_2$ respond differently to the two types of transitions, we suggest that DO/AIM events and glacial terminations may have a similar influence on $N_2O$ sources (and sinks). Since $N_2O$ concentrations may mainly reflect changes in marine and/or terrestrial emissions from low latitudes, in contrast to $CH_4$ and $CO_2$ emission changes which are also influenced by processes located at high latitudes, we speculate that high latitudes could account for the distinction of DO/AIM events and glacial terminations. Nevertheless,

the tropics may strongly support large climate variations by large emissions of greenhouse gases. Explaining why climate does not enter an interglacial after DO/AIM events, in particular after the transition from MIS 4 to 3, could reveal crucial information about the mechanisms at play during glacial terminations.

## Acknowledgments

We thank Dieter Lüthi for his support in assembling $CO_2$ records and Eric Wolff for his helpful comments on an earlier version of this manuscript. We benefited a lot from detailed and useful comments of two anonymous reviewers. This work, which is a contribution to the North Greenland Ice Core Project (NGRIP), the Talos Dome Ice Core Project (TALDICE) and the European Project for Ice Coring in Antarctica (EPICA), was supported by the University of Bern, the Swiss National Science Foundation, and the Prince Albert II of Monaco Foundation. NGRIP is directed and organized by the Department of Geophysics at the Niels Bohr Institute for Astronomy, Physics and Geophysics, University of Copenhagen, and it is supported by funding agencies in Denmark (SNF), Belgium (FNRS-CFB), France (IPEV and INSU/CNRS), Germany (AWI), Iceland (RANNIS), Japan (MEXT), Sweden (SPRS), Switzerland (SNF) and the United States of America (NSF, Office of Polar Programs). TALDICE, a joint European programme, is funded by national contributions from Italy, France, Germany, Switzerland and the United Kingdom. Primary logistical support was provided by PNRA at Talos Dome. EPICA, a joint European Science Foundation/European Commission scientific program, is funded by the European Commission and by national contributions from Belgium, Denmark, France, Germany, Italy, the Netherlands, Norway, Sweden, Switzerland and the United Kingdom. The main logistic support was provided by IPEV/PNRA at Dome C and AWI at Dronning Maud Land. This is TALDICE publication no 8 and EPICA publication no 272.

## Appendix A

### *A.1. Measurement technique for $N_2O$ and $CH_4$*

Following the extraction of ancient air from polar ice samples of about 40 g (University of Bern) or 50 g (Laboratoire de Glaciologie et Géophysique de l'Environnement, LGGE) by a melt–refreezing method, the air is injected into a sampling loop and analyzed for $N_2+O_2+Ar$, $CH_4$ (University of Bern and LGGE) and $N_2O$ (University of Bern) by gas chromatography. The gas chromatographs are equipped with a thermal conductivity detector (TCD, for $N_2+O_2+Ar$), a flame ionization detector (FID, for $CH_4$) and an electron capture detector (ECD, for $N_2O$). See e.g. Flückiger et al. (2004) and Chappellaz et al. (1997) for detailed descriptions of the melt–refreezing method and the measurement systems. Parts of the $N_2O$ and $CH_4$ records were measured with a slightly modified measurement system at the University of Bern. This modified system allows for up to 16 measurements per day (instead of up to 8 measurements per day with the unmodified system). The melt–refreezing air extraction method is unchanged. However, with the modified system we perform one single injection per sample instead of three injections with the unmodified system. The amount of analyzed air remains the same, since we now inject the air into a three times larger sampling loop. While with the unmodified system $CH_4$ and $N_2O$ are cryofocused on one trap (at −196 °C) each, the two gases are now split by Y-splitters after a first chromatographic separation and then cryofocused on three traps each. Since the traps are heated up with some time lag, there are still three peaks in both, the FID and ECD. Both systems produce similar results, as indicated by remeasurements of previously measured samples along the TD ice core (adjacent depth levels, concentrations spanning the whole natural range). 86 reanalysed samples for $CH_4$ reveal a median of the differences (remeasurements with modified system minus previous measurements with unmodified system) of −1.3 ppbv with a 95% confidence interval of [−3.0, 0.7] ppbv. 59 reanalysed samples for $N_2O$ reveal a median of the differences of −1.7 ppbv with a 95% confidence interval of [−3.3, 0.3] ppbv. In respect of the median of the differences, the unmodified and the modified system are, thus, statistically undistinguishable for both, $CH_4$ and $N_2O$ concentrations.

In previous studies, the uncertainty of $N_2O$ measurements has been determined by the square root of the sum of the squared standard deviation of measurements of bubble-free ice with standard gas and the squared standard deviation of the three measurements of each sample, multiplied by the corresponding t-value of the t-distribution due to the small statistics (Flückiger et al., 2004). The uncertainties calculated according to Flückiger et al. (2004) average to 3.8 ppbv and 3.9 ppbv for our new NGRIP record covering the DO events 17 to 15 and our new TD record, respectively. Along the TD ice core, however, we checked the reproducibility of $N_2O$ measurements by series of five adjacent samples at nine different depth levels (Fig. 3). Overall, these measurements reveal a standard deviation of 5.6 ppbv with a 95% confidence interval of [4.6, 7.1] ppbv. Measuring adjacent samples may be the most reliable way to determine the reproducibility of our measurement system, since this method is based on measurements of air extracted from natural ice samples. The new measurements of adjacent samples indicate that the uncertainty could be slightly larger than estimated according to Flückiger et al. (2004). While we still use the latter uncertainty for the NGRIP record (due to missing measurements of adjacent samples along this ice core), we use the uncertainty based on measurements of adjacent samples for the TD $N_2O$ record.

Along the TD ice core, the scatter of five adjacent samples during intervals with dust concentrations above and below the threshold of 300 ppbw is statistically indistinguishable. This observation further increases our confidence in MIS 2 $N_2O$ concentrations measured along the TD ice core. However, we admit that series of adjacent samples may not be unambiguous to detect potential artefacts, since a similar series of adjacent samples along the EDML ice core revealed high concentrations apparently subject to in situ production of $N_2O$, but the measurements also did not show a large scatter.

### *A.2. Offset corrections for $N_2O$ and $CH_4$ measurements*

According to Spahni et al. (2005) we correct $N_2O$ records measured at the University of Bern since the year 2003 by +10 ppbv in order to reach consistency with earlier records. This systematic offset of still unknown origin was determined by resampling EDC Holocene ice and by a comparison of the EDC and EDML Holocene $N_2O$ records (Spahni et al., 2005). From the records used for the composite $N_2O$ record (Fig. 1) the whole EDML and TD records, as well as the EDC record older than 40 kyr BP and the NGRIP record covering the DO events 17 to 15 are corrected by +10 ppbv. All other $N_2O$ records have been measured before the shift occurred and are thus uncorrected. The offset correction was recently verified by remeasurements along the EDC and NGRIP ice cores. Along the EDC ice core, 74 remeasurements covering MIS 15, 5 and 3, as well as the Holocene were performed (Schilt et al., 2010). Although some inconsistencies between earlier measurements and remeasurements were observed during MIS 3, the remeasurements overall clearly indicated that the $N_2O$ measurements performed at the University of Bern over many years are on a consistent reference scale, once the shift of 10 ppbv is taken into account (see Schilt et al., 2010 for more details). In order to cross-check the $N_2O$ measurements performed at the University of Bern with measurements from a different lab, we compare all Bern measurements with the GISP2 $N_2O$ record of Sowers et al. (2003). Figure 7 shows the GISP2 $N_2O$ record together with all Bern data from different ice cores (see also Fig. 1) put on the EDC3 time scale by $CH_4$ synchronisation (Appendix A.4). We calculate the differences between the GISP2 $N_2O$ data and the corresponding values of a smoothing spline through the Bern $N_2O$ data with a cutoff period of 1000 yr according to Enting (1987). The mean of the differences is

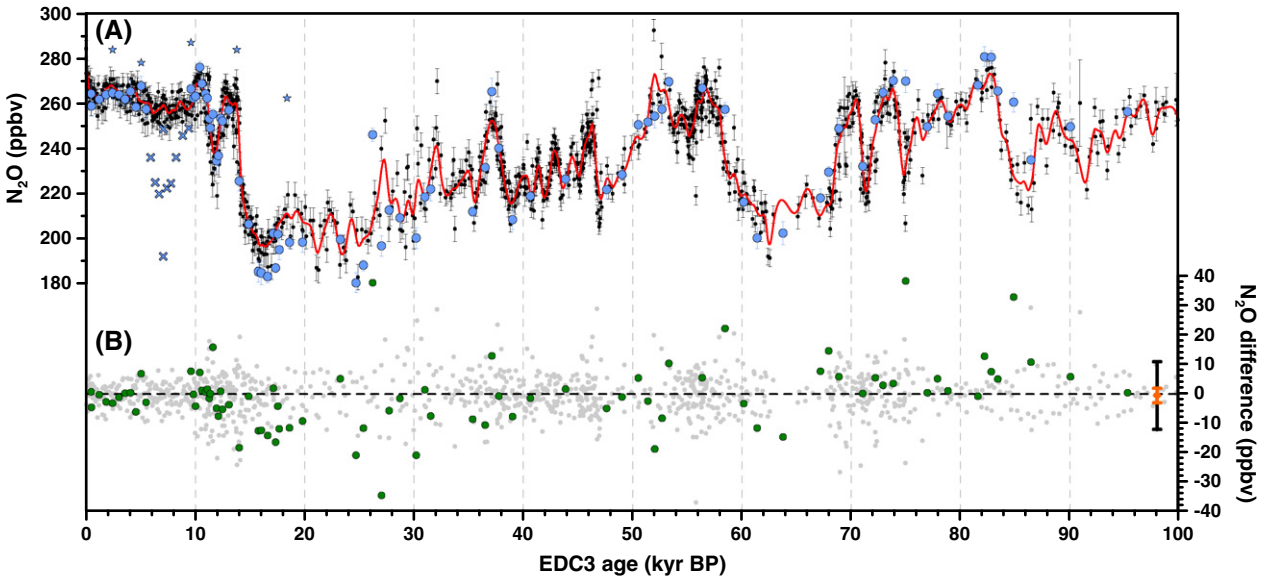


**Fig. 7.** Comparison of Bern $N_2O$ data with GISP2 $N_2O$ data of Sowers et al. (2003). (A) Black: $N_2O$ data measured at the University of Bern along different ice cores (see Fig. 1). Red: smoothing spline with a cutoff period of 1000 yr calculated according to Enting (1987) through the Bern $N_2O$ data. In contrast to the smoothing spline in Figure 1, this smoothing spline does not include the GISP2 $N_2O$ data. Blue: GISP2 $N_2O$ data (Sowers et al., 2003). Crosses indicate values which are biased by the extraction process. Stars indicate values which we assume to be affected by artefacts. All data are shown on the ($CH_4$ synchronised) EDC3 time scale (Appendix A.4) (B). Green: differences between GISP2 $N_2O$ data and the smoothing spline calculated through the Bern $N_2O$ data. Grey: differences between Bern $N_2O$ data and the smoothing spline calculated through the Bern $N_2O$ data. The orange diamond on the right shows the mean of the differences between GISP2 $N_2O$ data and the smoothing spline calculated through the Bern $N_2O$ data, with the orange error bar indicating the 95% confidence interval of the mean and the black error bar indicating the standard deviation of the differences. Note that this standard deviation does not correspond to the reproducibility of the measurement system (see Appendix A.2).

−0.5 ppbv with a 95% confidence interval of [−2.9, 1.9] ppbv. The differences between GISP2 and Bern data have a standard deviation of 11.5 ppbv. We note that the scattering of Bern data around the smoothing spline calculated through the Bern data is of the same order (Fig. 7). Accordingly, the scattering, which is larger than the reproducibility of the measurement system at the University of Bern (see Appendix A.1), may at least partly be caused by the applied method using a smoothing spline. In addition, uncertainties in the $CH_4$ synchronisation may add to the differences between GISP2 and Bern data. The $CH_4$ synchronisation does for instance not exclude that the high GISP2 $N_2O$ value at around 26 kyr BP corresponds to the high TD values observed slightly earlier. Overall, the GISP2 $N_2O$ record is in very good agreement with the Bern data, and the comparison does not indicate a remaining systematic offset in the presented $N_2O$ composite record.

$CH_4$ records measured at LGGE are systematically lower than those measured at the University of Bern and are, therefore, corrected by +6 ppbv (Spahni et al., 2005).

### A.3. Measurement technique for dust

The dust concentration was measured with a laser based particle detector which has been described in detail in Ruth et al. (2002). The particle detector has been implemented in an established continuous flow analysis (CFA) system (e.g. Kaufmann et al., 2008; Röthlisberger et al., 2000), where ice core pieces of a cross section of 34 mm × 34 mm and 1 m length are melted continuously along the direction of the ice core. For decontamination reasons only the melt water of the inner of two concentric sections is pumped to the detectors. The dust concentration was recorded at an effective depth resolution of 1 cm (Ruth et al., 2002), however, we here use a smoothing spline with a cutoff period of 2000 yr (Enting, 1987). Gaps in the dust concentration record are due to wrongly calibrated or missing measurements. Note that for the depth interval of the brittle ice (667 to 1002 m) a partial contamination and, thus, too high dust concentrations cannot completely be ruled out. However, this does not affect the conclusions of this study.

### A.4. Time scale synchronisation

In order to establish composite records consisting of $CO_2$ and $N_2O$ measurements from different ice cores a common time scale is needed. We use the EDC3 gas age scale (Loulergue et al., 2007) as a reference and match the gas records of all other ice cores to this time scale. $CH_4$ is most suited for such synchronisation, since it is globally well mixed and shows rapid and large natural variations synchronous in all ice cores (Blunier et al., 1998, 2007). Along the EDC $CH_4$ record back to 140 kyr BP, we define 47 tie points which represent characteristic events (Fig. 1). Identification of the tie points in the $CH_4$ records of all other ice cores and subsequent synchronisation to the EDC ice core leads to the desired common time scale. In order to determine the depth of the tie points we sometimes interpolate (on the depth scale) to the corresponding $CH_4$ concentration. The age is linearly interpolated in-between the tie points and linearly extrapolated at the beginnings and ends of fragmentary $CH_4$ records. For TD between 50 and 140 kyr BP we use the TALDICE1 time scale (Buiron et al., 2010), since TALDICE1 has been built based on $CH_4$ synchronisation to the EDC3 time scale for this time interval. Since the time resolution of the Taylor Dome $CH_4$ record is not adequate for some time intervals, we directly synchronise the Taylor Dome $CO_2$ record to the Byrd $CO_2$ record.

## Appendix B. Supplementary data

Files containing new $N_2O$ and $CH_4$ data from the TD, NGRIP and EDML ice cores, as well as the smoothing splines of the composite greenhouse gas records are linked to the online version of this paper at doi:10.1016/j.epsl.2010.09.027. The ice core records can also be downloaded from the website of the World Data Center for Paleoclimatology at www.ncdc.noaa.gov/paleo.

## References


Ahn, J., Brook, E.J., 2007. Atmospheric $CO_2$ and climate from 65 to 30 ka B.P. Geophys. Res. Lett. 34.

Ahn, J., Brook, E.J., 2008. Atmospheric $CO_2$ and climate on millennial time scales during the last glacial period. Science 322, 83–85.

Berrittella, C., van Huissteden, J., 2009. Uncertainties in modelling $CH_4$ emissions from northern wetlands in glacial climates: effect of hydrological model and $CH_4$ model structure. Clim. Past 5, 361–373.

Blunier, T., Chappellaz, J., Schwander, J., Dällenbach, A., Stauffer, B., Stocker, T.F., Raynaud, D., Jouzel, J., Clausen, H.B., Hammer, C.U., Johnsen, S.J., 1998. Asynchrony of Antarctic and Greenland climate change during the last glacial period. Nature 394, 739–743.

Blunier, T., Spahni, R., Barnola, J.M., Chappellaz, J., Loulergue, L., Schwander, J., 2007. Synchronization of ice core records via atmospheric gases. Clim. Past 3, 325–330.

Bock, M., Schmitt, J., Möller, L., Spahni, R., Blunier, T., Fischer, H., 2010. Hydrogen isotopes preclude marine hydrate $CH_4$ emissions at the onset of Dansgaard-Oeschger events. Science 328, 1686–1689.

Bond, G., Broecker, W., Johnsen, S., McManus, J., Labeyrie, L., Jouzel, J., Bonani, G., 1993. Correlations between climate records from North-Atlantic sediments and Greenland ice. Nature 365, 143–147.

Bouwman, A.F., Fung, I., Matthews, E., John, J., 1993. Global analysis of the potential for $N_2O$ production in natural soils. Glob. Biogeochem. Cycles 7, 557–597.

Broecker, W.S., 1998. Paleocean circulation during the Last Deglaciation: a bipolar seesaw? Paleoceanography 13, 119–121.

Brook, E.J., Harder, S., Severinghaus, J., Steig, E.J., Sucher, C.M., 2000. On the origin and timing of rapid changes in atmospheric methane during the last glacial period. Glob. Biogeochem. Cycles 14, 559–572.

Brook, E.J., Sowers, T., Orchardo, J., 1996. Rapid variations in atmospheric methane concentration during the past 110,000 years. Science 273, 1087–1091.

Bubier, J.L., Moore, T.R., 1994. An ecological perspective on methane emissions from northern wetlands. Trends Ecol. Evol. 9, 460–464.

Buiron, D., Chappellaz, J., Stenni, B., Frezzotti, M., Baumgartner, M., Capron, E., Landais, A., Lemieux-Dudon, B., Masson-Delmotte, V., Montagnat, M., Parrenin, F., Schilt, A., 2010. TALDICE-1 age scale of the Talos Dome deep ice core, East Antarctica. Clim. Past Discus. 6, 1733–1776.

Capron, E., Landais, A., Lemieux-Dudon, B., Schilt, A., Masson-Delmotte, V., Buiron, D., Chappellaz, J., Dahl-Jensen, D., Johnsen, S., Leuenberger, M., Loulergue, L., Oerter, H., 2010. Synchronising EDML and NorthGRIP ice cores using $\delta^{18}O$ of atmospheric oxygen ($\delta^{18}O_{atm}$) and $CH_4$ measurements over MIS 5 (80–123 ka). Quatern. Sci. Rev. 29, 222–234.

Chappellaz, J., Barnola, J.M., Raynaud, D., Korotkevich, Y.S., Lorius, C., 1990. Ice-core record of atmospheric methane over the past 160,000 years. Nature 345, 127–131.

Chappellaz, J., Blunier, T., Kints, S., Dällenbach, A., Barnola, J.M., Schwander, J., Raynaud, D., Stauffer, B., 1997. Changes in the atmospheric $CH_4$ gradient between Greenland and Antarctica during the Holocene. J. Geophys. Res. Atmos. 102, 15987–15997.

Chappellaz, J., Blunier, T., Raynaud, D., Barnola, J.M., Schwander, J., Stauffer, B., 1993. Synchronous changes in atmospheric $CH_4$ and Greenland climate between 40 kyr and 8 kyr BP. Nature 366, 443–445.

Crutzen, P.J., Bruhl, C., 1993. A model study of atmospheric temperatures and the concentrations of ozone, hydroxyl, and some other photochemically active gases during the glacial, the preindustrial Holocene and the present. Geophys. Res. Lett. 20, 1047–1050.

Dällenbach, A., Blunier, T., Flückiger, J., Stauffer, B., Chappellaz, J., Raynaud, D., 2000. Changes in the atmospheric $CH_4$ gradient between Greenland and Antarctica during the Last Glacial and the transition to the Holocene. Geophys. Res. Lett. 27, 1005–1008.

Dansgaard, W., Johnsen, S.J., Clausen, H.B., Dahl-Jensen, D., Gundestrup, N.S., Hammer, C.U., Hvidberg, C.S., Steffensen, J.P., Sveinbjörnsdottir, A.E., Jouzel, J., Bond, G., 1993. Evidence for general instability of past climate from a 250-kyr ice-core record. Nature 364, 218–220.

Dansgaard, W., Johnsen, S.J., Clausen, H.B., Dahl-Jensen, D., Gundestrup, N.S., Hammer, C.U., Oeschger, H., 1984. North Atlantic climatic oscillations revealed by deep Greenland ice cores. In: Hansen, J.E., Takahashi, T. (Eds.), Climate Processes and Climate Sensitivity. American Geophysical Union, Washington, D.C.

Denton, G.H., Alley, R.B., Comer, G.C., Broecker, W.S., 2005. The role of seasonality in abrupt climate change. Quatern. Sci. Rev. 24, 1159–1182.

Emmer, E., Thunell, R.C., 2000. Nitrogen isotope variations in Santa Barbara Basin sediments: implications for denitrification in the eastern tropical North Pacific during the last 50,000 years. Paleoceanography 15, 377–387.

Enting, I.G., 1987. On the use of smoothing splines to filter $CO_2$ data. J. Geophys. Res. 92, 10977–10984.

EPICA Community Members, 2006. One-to-one coupling of glacial climate variability in Greenland and Antarctica. Nature 444, 195–198.

Fischer, H., Behrens, M., Bock, M., Richter, U., Schmitt, J., Loulergue, L., Chappellaz, J., Spahni, R., Blunier, T., Leuenberger, M., Stocker, T.F., 2008. Changing boreal methane sources and constant biomass burning during the last termination. Nature 452, 864–867.

Flückiger, J., Blunier, T., Stauffer, B., Chappellaz, J., Spahni, R., Kawamura, K., Schwander, J., Stocker, T.F., Dahl-Jensen, D., 2004. $N_2O$ and $CH_4$ variations during the last glacial epoch: insight into global processes. Glob. Biogeochem. Cycles 18, GB1020. doi:10.1029/2003GB002122.

Flückiger, J., Dällenbach, A., Blunier, T., Stauffer, B., Stocker, T.F., Raynaud, D., Barnola, J.M., 1999. Variations in atmospheric $N_2O$ concentration during abrupt climatic changes. Science 285, 227–230.

Flückiger, J., Monnin, E., Stauffer, B., Schwander, J., Stocker, T.F., Chappellaz, J., Raynaud, D., Barnola, J.M., 2002. High-resolution Holocene $N_2O$ ice core record and its relationship with $CH_4$ and $CO_2$. Glob. Biogeochem. Cycles 16, 1010. doi:10.1029/2001 GB001417.

Hays, J.D., Imbrie, J., Shackleton, N.J., 1976. Variations in Earth's orbit — pacemaker of Ice Ages. Science 194, 1121–1132.

Huber, C., Leuenberger, M., Spahni, R., Flückiger, J., Schwander, J., Stocker, T.F., Johnsen, S., Landais, A., Jouzel, J., 2006. Isotope calibrated Greenland temperature record over Marine Isotope Stage 3 and its relation to $CH_4$. Earth Planet. Sci. Lett. 243, 504–519.

Indermühle, A., Monnin, E., Stauffer, B., Stocker, T.F., Wahlen, M., 2000. Atmospheric $CO_2$ concentration from 60 to 20 kyr BP from the Taylor Dome ice core, Antarctica. Geophys. Res. Lett. 27, 735–738.

Johnsen, S.J., Dahl-Jensen, D., Gundestrup, N., Steffensen, J.P., Clausen, H.B., Miller, H., Masson-Delmotte, V., Sveinbjornsdottir, A.E., White, J., 2001. Oxygen isotope and palaeotemperature records from six Greenland ice-core stations: Camp Century, Dye-3, GRIP, GISP2, Renland and NorthGRIP. J. Quatern. Sci. 16, 299–307.

Kaplan, J.O., Folberth, G., Hauglustaine, D.A., 2006. Role of methane and biogenic volatile organic compound sources in late glacial and Holocene fluctuations of atmospheric methane concentrations. Glob. Biogeochem. Cycles 20.

Kaufmann, P.R., Federer, U., Hutterli, M.A., Bigler, M., Schüpbach, S., Ruth, U., Schmitt, J., Stocker, T.F., 2008. An improved continuous flow analysis system for high-resolution field measurements on ice cores. Environ. Sci. Technol. 42, 8044–8050.

Khalil, M.A.K., Rasmussen, R.A., Shearer, M.J., 2002. Atmospheric nitrous oxide: patterns of global change during recent decades and centuries. Chemosphere 47, 807–821.

Kroeze, C., Mosier, A., Bouwman, L., 1999. Closing the global $N_2O$ budget: a retrospective analysis 1500–1994. Glob. Biogeochem. Cycles 13, 1–8.

Lambert, F., Delmonte, B., Petit, J.R., Bigler, M., Kaufmann, P.R., Hutterli, M.A., Stocker, T.F., Ruth, U., Steffensen, J.P., Maggi, V., 2008. Dust-climate couplings over the past 800,000 years from the EPICA Dome C ice core. Nature 452, 616–619.

Landais, A., Masson-Delmotte, V., Nebout, N.C., Jouzel, J., Blunier, T., Leuenberger, M., Dahl-Jensen, D., Johnsen, S., 2007. Millenial scale variations of the isotopic composition of atmospheric oxygen over Marine Isotopic Stage 4. Earth Planet. Sci. Lett. 258, 101–113.

Leuenberger, M., Siegenthaler, U., 1992. Ice-age atmospheric concentration of nitrous-oxide from an Antarctic ice core. Nature 360, 449–451.

Liu, D., Wang, Y., Cheng, H.R., Lawrence, E., Kong, X., Wang, X., Hardt, B., Wu, J., Chen, S., Jiang, X., He, Y., Dong, J., Zhao, K., 2010. Sub-millennial variability of Asian monsoon intensity during the early MIS 3 and its analogue to the ice age terminations. Quatern. Sci. Rev. 29, 1107–1115.

Loulergue, L., Parrenin, F., Blunier, T., Barnola, J.M., Spahni, R., Schilt, A., Raisbeck, G., Chappellaz, J., 2007. New constraints on the gas age-ice age difference along the EPICA ice cores, 0–50 kyr. Clim. Past 3, 527–540.

Loulergue, L., Schilt, A., Spahni, R., Masson-Delmotte, V., Blunier, T., Lemieux, B., Barnola, J.M., Raynaud, D., Stocker, T.F., Chappellaz, J., 2008. Orbital and millennial-scale features of atmospheric CH4 over the past 800,000 years. Nature 453, 383–386.

Lüthi, D., Le Floch, M., Bereiter, B., Blunier, T., Barnola, J.M., Siegenthaler, U., Raynaud, D., Jouzel, J., Fischer, H., Kawamura, K., Stocker, T.F., 2008. High-resolution carbon dioxide concentration record 650,000–800,000 years before present. Nature 453, 379–382.

Machida, T., Nakazawa, T., Fujii, Y., Aoki, S., Watanabe, O., 1995. Increase in the atmospheric nitrous-oxide concentration during the last 250 years. Geophys. Res. Lett. 22, 2921–2924.

Martinerie, P., Brasseur, G.P., Granier, C., 1995. The chemical-composition of ancient atmospheres — a model study constrained by ice core data. J. Geophys. Res. Atmos. 100, 14291–14304.

Masson-Delmotte, V., Jouzel, J., Landais, A., Stievenard, M., Johnsen, S.J., White, J.W.C., Werner, M., Sveinbjornsdottir, A., Fuhrer, K., 2005. GRIP deuterium excess reveals rapid and orbital-scale changes in Greenland moisture origin. Science 309, 118–121.

Minschwaner, K., Carver, R.W., Briegleb, B.P., Roche, A.E., 1998. Infrared radiative forcing and atmospheric lifetimes of trace species based on observations from UARS. J. Geophys. Res. Atmos. 103, 23243–23253.

Miteva, V., Sowers, T., Brenchley, J., 2007. Production of $N_2O$ by ammonia oxidizing bacteria at subfreezing temperatures as a model for assessing the $N_2O$ anomalies in the Vostok ice core. Geomicrobiol. J. 24, 451–459.

Monnin, E., Indermühle, A., Dällenbach, A., Flückiger, J., Stauffer, B., Stocker, T.F., Raynaud, D., Barnola, J.M., 2001. Atmospheric $CO_2$ concentrations over the last glacial termination. Science 291, 112–114.

Monnin, E., Steig, E.J., Siegenthaler, U., Kawamura, K., Schwander, J., Stauffer, B., Stocker, T.F., Morse, D.L., Barnola, J.M., Bellier, B., Raynaud, D., Fischer, H., 2004. Evidence for substantial accumulation rate variability in Antarctica during the Holocene, through synchronization of $CO_2$ in the Taylor Dome, Dome C and DML ice cores. Earth Planet. Sci. Lett. 224, 45–54.

Nevison, C.D., Weiss, R.F., Erickson, D.J., 1995. Global oceanic emissions of nitrous-oxide. J. Geophys. Res. Oceans 100, 15809–15820.

NGRIP Members, 2004. High-resolution record of Northern Hemisphere climate extending into the last interglacial period. Nature 431, 147–151.

Pepin, L., Raynaud, D., Barnola, J.M., Loutre, M.F., 2001. Hemispheric roles of climate forcings during glacial–interglacial transitions as deduced from the Vostok record and LLN-2D model experiments. J. Geophys. Res. Atmos. 106, 31885–31892.

Petit, J.R., Jouzel, J., Raynaud, D., Barkov, N.I., Barnola, J.M., Basile, I., Bender, M., Chappellaz, J., Davis, M., Delaygue, G., Delmotte, M., Kotlyakov, V.M., Legrand, M., Lipenkov, V.-Y., Lorius, C., Pepin, L., Ritz, C., Saltzmann, E., Stievenard, M., 1999. Climate and atmospheric history of the past 420,000 years from the Vostok ice core, Antarctica. Nature 399, 429–436.

Ramaswamy, V., Boucher, O., Haigh, J., Hauglustaine, D., Haywood, J., Myhre, G., Nakajima, T., Shi, G.Y., Solomon, S., 2001. Radiative forcing of climate change. In:

Houghton, J.T., Ding, Y., Griggs, D.J., Noguer, M., van der Linden, P.J., Dai, X., Maskell, K., Johnson, C.A. (Eds.), Climate Change 2001: The Scientific Basis. Contribution of Working Group I to the Third Assessment Report of the Intergovernmental Panel on Climate Change. Cambridge Univ. Press, Cambridge.

Rohde, R.A., Price, P.B., Bay, R.C., Bramall, N.E., 2008. In situ microbial metabolism as a cause of gas anomalies in ice. Proc. Natl Acad. Sci. USA 105, 8667–8672.

Röthlisberger, R., Bigler, M., Hutterli, M., Sommer, S., Stauffer, B., Junghans, H.G., Wagenbach, D., 2000. Technique for continuous high-resolution analysis of trace substances in firn and ice cores. Environ. Sci. Technol. 34, 338–342.

Ruth, U., Wagenbach, D., Bigler, M., Steffensen, J.P., Röthlisberger, R., Miller, H., 2002. High-resolution microparticle profiles at NorthGRIP, Greenland: case studies of the calcium–dust relationship. Ann. Glaciol. 35, 237–242.

Ruth, U., Barnola, J.M., Beer, J., Bigler, M., Blunier, T., Castellano, E., Fischer, H., Fundel, F., Huybrechts, P., Kaufmann, P., Kipfstuhl, S., Lambrecht, A., Morganti, A., Oerter, H., Parrenin, F., Rybak, O., Severi, M., Udisti, R., Wilhelms, F., Wolff, E., 2007. "EDML1": a chronology for the EPICA deep ice core from Dronning Maud Land, Antarctica, over the last 150 000 years. Clim. Past 3, 475–484.

Schilt, A., Baumgartner, M., Blunier, T., Schwander, J., Spahni, R., Fischer, H., Stocker, T.F., 2010. Glacial–interglacial and millennial-scale variations in the atmospheric nitrous oxide concentration during the last 800,000 years. Quatern. Sci. Rev. 29, 182–192.

Schmittner, A., Galbraith, E.D., 2008. Glacial greenhouse-gas fluctuations controlled by ocean circulation changes. Nature 456, 373–376.

Schwander, J., Sowers, T., Barnola, J.M., Blunier, T., Fuchs, A., Malaize, B., 1997. Age scale of the air in the summit ice: implication for glacial–interglacial temperature change. J. Geophys. Res. Atmos. 102, 19483–19493.

Severinghaus, J.P., Beaudette, R., Headly, M.A., Taylor, K., Brook, E.J., 2009. Oxygen-18 of $O_2$ records the impact of abrupt climate change on the terrestrial biosphere. Science 324, 1431–1434.

Sowers, T., 2001. $N_2O$ record spanning the penultimate deglaciation from the Vostok ice core. J. Geophys. Res. Atmos. 106, 31903–31914.

Sowers, T., Alley, R.B., Jubenville, J., 2003. Ice core records of atmospheric $N_2O$ covering the last 106,000 years. Science 301, 945–948.

Spahni, R., Chappellaz, J., Stocker, T.F., Loulergue, L., Hausammann, G., Kawamura, K., Flückiger, J., Schwander, J., Raynaud, D., Masson-Delmotte, V., Jouzel, J., 2005. Atmospheric methane and nitrous oxide of the late Pleistocene from Antarctic ice cores. Science 310, 1317–1321.

Stauffer, B., Flückiger, J., Monnin, E., Schwander, J., Barnola, J.M., Chappellaz, J., 2002. Atmospheric $CO_2$, $CH_4$ and $N_2O$ records over the past 60,000 years based on the comparison of different polar ice cores. Ann. Glaciol. 35, 202–208.

Stenni, B., Buiron, D., Frezzotti, M., Albani, S., Barbante, C., Bard, E., Barnola, J.M., Baroni, M., Baumgartner, M., Bonazza, M., Capron, E., Castellano, E., Chappellaz, J., Delmonte, B., Falourd, S., Genoni, L., Iacumin, P., Jouzel, J., Kipfstuhl, J., Landais, A., Lemieux-Dudon, B., Maggi, V., Masson-Delmotte, V., Mazzola, C., Minster, B., Montagnat, M., Mulvaney, R., Narcisi, B., Oerter, H., Parrenin, F., Petit, J. R., Ritz, C., Scarchilli, C., Schilt, A., Schüpbach, S., Schwander, J., Selmo, E., Severi, M., Stocker, T.F., Udisti, R., submitted for publication. The expression of the bipolar climate seesaw around Antarctica during the last deglaciation. Nature Geoscience.

Stocker, T.F., 1998. Climate change — the seesaw effect. Science 282, 61–62.

Stocker, T.F., Johnsen, S.J., 2003. A minimum thermodynamic model for the bipolar seesaw. Paleoceanography 18, 1087. doi:10.1029/2003PA00092.

Suthhof, A., Ittekkot, V., Gaye-Haake, B., 2001. Millennial-scale oscillation of denitrification intensity in the Arabian Sea during the late Quaternary and its potential influence on atmospheric $N_2O$ and global climate. Glob. Biogeochem. Cycles 15, 637–649.

Voelker, A.H.L., 2002. Global distribution of centennial-scale records for Marine Isotope Stage (MIS) 3: a database. Quatern. Sci. Rev. 21, 1185–1212.

Volk, C.M., Elkins, J.W., Fahey, D.W., Dutton, G.S., Gilligan, J.M., Loewenstein, M., Podolske, J.R., Chan, K.R., Gunson, M.R., 1997. Evaluation of source gas lifetimes from stratospheric observations. J. Geophys. Res. Atmos. 102, 25543–25564.

WMO, 2009. WMO Greenhouse Gas Bulletin, No. 5. The State of Greenhouse Gases in the Atmosphere Using Global Observations through 2008. World Meteorological Organization. 4 pp.

Wolff, E.W., Fischer, H., Röthlisberger, R., 2009. Glacial terminations as southern warmings without northern control. Nat. Geosci. 2, 206–209.